Electronic and structural properties of sodium clusters

José Luís Martins* and Jean Buttet
Institut de Physique Expérimentale, Ecole Polytechnique Fédérale de Lausanne, 1015 Lausanne, Switzerland

Roberto Car
International School for Advanced Studies, Strada Costiera 11, Trieste, Italy
(Received 27 August 1984)

We present an investigation of the structural and electronic properties of the sodium clusters Na_n and Na_n^+ with $n \leq 8$ and $n = 13$, based on self-consistent pseudopotential local-spin-density calculations. In order to obtain the equilibrium geometries without imposing any symmetry constraint, we start from randomly generated cluster geometries and let them relax under the action of the forces on the atoms, which are derived from the Hellmann-Feynman theory. We find that the clusters with up to five atoms have planar equilibrium geometries, the six-atom cluster is quasiplanar, and real three-dimensional structures only begin to occur when the number of atoms is greater than or equal to seven. We compare our results with recently obtained experimental data and find good agreement with the measured photoionization appearance potentials and the electron-spin-resonance spectra. Metallic bonding is the dominant feature of our calculated electronic structures and we show that the equilibrium geometries can be explained with a simple model having the delocalized nature of the metallic electrons and the Jahn-Teller effect as basic ingredients.

I. INTRODUCTION

The geometrical structure of metal aggregates or clusters is certainly, in many cases, different from the bulk metal structure. It has, for example, been shown[1] that Ag and Au clusters with diameters between 20 and 100 Å are not single crystals, but are composed of tetrahedral units separated by twin planes and have a fivefold symmetry axis. The structure of very small metal clusters or microclusters is also expected to be different from the highly symmetrical bulk structures, and it is not correct to build the microclusters from bulk unit cells, as has been very often assumed in model calculations.

A good knowledge of the geometry of small clusters is important in order to understand in detail the evolution of different properties as the size of the clusters grows and thus to bridge the gap between the atomic and bulk properties of matter. Furthermore, some important applications of metal aggregates, such as catalytic reactions[2] and latent image formation in the photographic process,[3] certainly depend not only on their size but also on their geometrical and electronic structure.

The experimental information available on the geometrical structure of metallic clusters of the order of ten atoms is indirect, and in most cases not even the symmetries are known. Any calculation of the physical properties of microclusters must either assume a reasonable geometrical structure or try to predict the geometry from the minimization of the calculated total energy. In the case of dimers, where only the interatomic distance has to be adjusted, the optimization of the geometry is not a main problem, but in the case of trimers the calculation of the whole Born-Oppenheimer surface already requires a very large number of single geometry calculations.[4,5] For larger clusters with n atoms, where the geometry is described by $3n-6$ parameters, it is impossible to calculate the whole Born-Oppenheimer surface and it becomes difficult to find the true energy minimum. In most cases the energy minimization is carried out only with respect to a couple of parameters, the others being kept constant or fixed by the symmetry constraints. The most symmetrical configurations of the very small clusters are, however, very often unstable due to the Jahn-Teller effect. The calculations that only consider highly symmetrical geometries often miss the true equilibrium geometry.

In this paper we calculate the equilibrium configurations of very small clusters without making any *a priori* assumption. We start from a randomly generated initial geometry and subsequently let the cluster relax under the action of the forces on the atoms until an equilibrium configuration is reached. To avoid being trapped in a local minimum, we repeat the process with different initial geometries.

For a given atomic configuration the electronic charge density and the total energy of a cluster are calculated self-consistently within the local-spin-density (LSD) approximation[6] of the density-functional theory.[7] We use a first-principles, norm-conserving pseudopotential[8,9] to treat the effect of the core electrons on the valence electrons. To obtain the forces on the atoms we follow a generalization of the Hellmann-Feynman theory[10] to the pseudopotential local-spin-density scheme.[11,12]

This method was used to determine the equilibrium structures and to calculate the electronic properties of the sodium clusters Na_n and Na_n^+, with $n \leq 8$ and $n = 13$. A preliminary account of this work was previously presented.[13]

The alkali aggregates are among the better known microclusters, both experimentally[14–23] and theoretically.[4,5,24–29] Using the molecular-beam technique to pro-

duce the clusters and the mass-spectrometry technique to detect clusters with a given number of atoms, several properties of sodium aggregates were measured, including the photoionization appearance potentials of Na_n clusters,[14–16] the two-photon ionization spectra of Na_3,[17,18] the laser-induced atomic fluorescence spectra of Na_3.[19] The electron-spin-resonance (ESR) spectra of matrix-isolated clusters have provided important information about the geometries of Na_3 and Na_7.[20,21] The optical absorption[22] and Raman[23] spectra have also been obtained for Na aggregates deposited in a frozen inert-gas matrix.

Several studies of alkali clusters beyond the Hartree-Fock level have been published, most concerning only dimers, trimers, and sometimes quadrimers. Some symmetrical configurations of the clusters Na_2 to Na_8 (Ref. 25) were studied with a Hartree-Fock method, which included in a non-self-consistent way a correction for the correlation energy in the local-density approximation, and which treated the cores in the pseudopotential scheme. Several geometries of Li_6 with the internuclear distance fixed at the bulk value,[27] the pentagonal bipyramidal geometries of the alkali septamers,[28] and some highly symmetric geometries of the Li_{13} cluster[29] were studied with a configuration interaction method which treated the Na and K cores in the pseudopotential approximation. However, all the calculations for clusters with more than three atoms have made some *a priori* assumptions on the geometry of the cluster. The local-density scheme has also been used recently to study metallic dimers[30,31] and the structure of copper clusters built from bulk unit cells.[32]

In this study of the structural and electronic properties of sodium clusters we find that clusters with six atoms or less have a planar or quasiplanar equilibrium geometry with a characteristic triangular pattern, whereas the larger clusters have three-dimensional structures in which all the atomic distances are similar. We calculate the adiabatic ionization potentials, the atomization and dissociation energies, and the electronic charge and spin density of the clusters. Where available, we find good agreement with the experimental data, in particular with the photoionization appearance potentials and the ESR results. We also present a detailed discussion of the calculated equilibrium structures and show that the main factor governing the ground-state geometries of the small clusters is the delocalized metallic nature of the valence electrons combined with the Jahn-Teller effect.

The paper is organized as follows: In Sec. II we give a brief account of the computational procedure, including the expression for the Hellmann-Feynman forces. In Sec. III we present the results, compare them with the available experimental data and discuss the trends with increasing particle size. A discussion of bonding and of its relation to the electronic and structural properties of the clusters is given in Sec. IV. Our conclusions are presented in Sec. V. Except when explicitly stated, atomic units ($e=\hbar=m_e=1$) are used in this work.

II. COMPUTATIONAL METHOD

As already mentioned, in our theoretical approach the core-electron effects on the valence electrons are treated within the pseudopotential approximation, whereas the exchange and correlation effects are treated self-consistently within the local-spin-density approximation[6] of the density-functional theory.[7]

We use an l-dependent, norm-conserving pseudopotential[8,9] derived from an *ab initio* atomic calculation performed in the local-density approximation. This pseudopotential has the form

$$\hat{V}_{\rm ps}=-\frac{Z}{r}\sum_{i=1}^{2}c_i\,\mathrm{erf}(\sqrt{\gamma_i}r)+\sum_{l=0}^{1}\left[\sum_{i=1}^{3}(a_i+b_i r^2)e^{-\alpha_i r^2}\right]\hat{P}_l\ .$$

Here $\hat{P}_l$ is the projection operator on the states of angular momentum l, and Z is the ionic charge. The constants c_i, γ_i, a_i, b_i, and α_i can be found in Ref. 9.

For the exchange and correlation energy $\epsilon_{\rm xc}^{\rm LSD}$ and potential $V_{{\rm xc},\sigma}^{\rm LSD}$ we use the interpolation formulas of Perdew and Zunger[33] derived from the Monte Carlo calculations for the homogeneous electron gas done by Ceperley and Alder.[34]

In this framework the ground-state electronic density of a molecule with n atoms and N valence electrons is obtained by solving the set of self-consistent equations,

$$\left[-\tfrac{1}{2}\nabla^2+\sum_{j=1}^{n}\hat{V}_{\rm ps}^{(j)}+V_H(\mathbf{r})+V_{{\rm xc},\sigma}^{\rm LSD}[\rho(\mathbf{r}),\xi(\mathbf{r})]\right]\phi_{i,\sigma}(\mathbf{r})=\epsilon_{i,\sigma}\phi_{i,\sigma}(\mathbf{r})$$

$$V_H(\mathbf{r})=\int d^3r'\frac{\rho(\mathbf{r}')}{|\mathbf{r}-\mathbf{r}'|},\quad \rho_\sigma(\mathbf{r})=\sum_i f_{i,\sigma}\,|\phi_{i,\sigma}(\mathbf{r})|^2\ , \tag{1}$$

$$\rho(\mathbf{r})=\rho_\uparrow(\mathbf{r})+\rho_\downarrow(\mathbf{r}),\quad \xi(\mathbf{r})=\frac{\rho_\uparrow(\mathbf{r})-\rho_\downarrow(\mathbf{r})}{\rho(\mathbf{r})}\ ,$$

where $\sigma=\uparrow,\downarrow$ is the index for up and down spins and $\hat{V}_{\rm ps}^{(j)}$ is the pseudopotential associated with the ion j, centered at the ionic site $\mathbf{R}^{(j)}$. The occupation numbers $f_{i,\sigma}$ are, respectively, equal to one or zero if $\epsilon_{i,\sigma}<\mu$ or $\epsilon_{i,\sigma}>\mu$, and are between one and zero if $\epsilon_{i,\sigma}=\mu$. The chemical potential μ is determined by the condition that the sum of the occupation numbers be equal to the number of valence electrons.

Using the self-consistent solutions of Eq. (1), the total pseudoenergy of the molecule is equal to

$$E(\mathbf{R}^{(1)},\ldots,\mathbf{R}^{(n)})=\sum_{j<k}\frac{Z_jZ_k}{|\mathbf{R}^{(j)}-\mathbf{R}^{(k)}|}+\sum_{\sigma=\uparrow,\downarrow}\sum_i f_{i,\sigma}\left\langle\phi_{i,\sigma}\left|-\tfrac{1}{2}\nabla^2+\sum_{j=i}^{n}\hat{V}_{\rm ps}^{(j)}+\tfrac{1}{2}V_H+\epsilon_{\rm xc}^{\rm LSD}(\rho,\xi)\right|\phi_{i,\sigma}\right\rangle . \quad (2)$$

If we apply the Hellmann-Feyman theory[10] to the energy expression [Eq. (2)], the force on atom j is given by[12,35]

$$F_\nu^{(j)}(\mathbf{R}^{(1)},\ldots,\mathbf{R}^{(n)})=-\frac{\partial}{\partial R_\nu^{(j)}}E(\mathbf{R}^{(1)},\ldots,\mathbf{R}^{(n)})$$

$$=\sum_{\sigma=\uparrow,\downarrow}\sum_i f_{i,\sigma}\left\langle\phi_{i,\sigma}\left|-\frac{\partial}{\partial R_\nu^{(j)}}\hat{V}_{\rm ps}^{(j)}\right|\phi_{i,\sigma}\right\rangle+\sum_{k\neq j}Z_kZ_j\frac{R_\nu^{(j)}-R_\nu^{(k)}}{|\mathbf{R}^{(j)}-\mathbf{R}^{(k)}|^3},\quad \nu=x,y,z . \quad (3)$$

It is well known that the Hellmann-Feynman forces are extremely sensitive to the quality of the basis set used in all electron calculations. As a matter of fact, the computation of the Hellmann-Feynman forces with the standard methods of quantum chemistry requires basis sets so large that the calculations are almost impractical.[36] In the case of a linear or combination of atomic orbitals (LCAO) basis set a reasonable convergence of the Hellmann-forces is only obtained when one adds to an initial basis set which gives a reasonably converged total energy, all the derivatives with respect to the nuclear positions of its basis functions.[37] However, if the basis set is independent of nuclear positions as in the floating orbital method for molecules or in the plane-wave basis set used in solid-state calculations, then the Hellmann-Feynman forces converge with increasing basis set size at the same rate as the total energy.[36]

The gradient of the calculated total energy can be calculated analytically if correction terms for the incompleteness of the basis set,[36] or even for the non-self-consistency[38] are added to the Hellmann-Feynman forces. Optimization of molecular geometries has been achieved using gradient forces.[36,39]

When a pseudopotential is used, only small basis sets are needed to calculate the total energy since it is not necessary to describe the core electron wave functions. If the pseudopotential does not have a divergence at the origin and the total pseudo charge density is smooth in the core region, the Hellmann-Feynman forces are less sensitive to the quality of the basis set.[35] Hellmann-Feynman forces have been used recently in pseudopotential calculations of solid and surface properties.[40]

To solve the self-consistent Kohn-Sham equations [Eq. (1)], we expand the molecular orbitals $\phi_{i,\sigma}$ in a linear combination of Gaussian atomic orbitals. A few words about our basis functions are necessary since we need a basis set not only to compute the total energy of a cluster as a function of the nuclear positions, but also to compute the Hellmann-Feynman forces on the nuclei. This is a much more difficult task than just to compute the total energy which is a variational quantity. The atomic $(3s,2p)$ Gaussian set (see Table I) that we have used in the present calculation has been optimized in order to give a sufficiently accurate description of the pseudo wave function, and gives Hellmann-Feynman forces which are, for all practical purposes, indistinguishable from the forces obtained by numerically differentiating the total energy.[35]

TABLE I. Exponents of the $(3s,2p)$ Gaussian basis set.

$3s$	0.030 466
	0.086 586
	0.397 668
$2p$	0.090 545
	0.634 653

As was first proposed by Sambe and Felton[41] we use an auxiliary set of Gaussian functions to fit the electronic charge density $\rho(\mathbf{r})$ and we calculate the electrostatic potential $V_H(\mathbf{r})$ using the fitted charge. Another set of Gaussian functions is used to fit the exchange and correlation energy $\epsilon_{\rm xc}^{\rm LSD}(\mathbf{r})$ and potential $V_{{\rm xc},\sigma}^{\rm LSD}(\mathbf{r})$, the exchange and correlation molecular integrals are then computed using the fitted functions. Several improvements on the original scheme of Sambe and Felton have been reported elsewhere.[4,42] For the sodium clusters our auxiliary sets include five even-tempered Gaussians at each atomic site and one Gaussian at the bonding site between each pair of nearest-neighbor atoms.

To obtain the equilibrium geometry of a cluster, we minimize its energy [Eq. (2)] with respect to the ionic positions using the information provided by the Hellmann-Feynman forces [Eq. (3)] and a steepest-descent method. At each step of the minimization process we perform a self-consistent calculation of the charge density, we evaluate the total energy $E(\mathbf{R}^{(I)})$ and the forces $\mathbf{F}^{(j)}(\mathbf{R}^{(I)})$ and we let the cluster geometry relax by a distance,

$$\Delta\mathbf{R}^{(j)}=\frac{1}{\alpha}\mathbf{F}^{(j)} .$$

The minimization is rapidly achieved if α is of the same order of magnitude as the largest eigenvalue of the matrix of the second derivatives of $E(\mathbf{R}^{(I)})$. For sodium clusters this corresponds to a vibrational frequency of $\sim 150\ {\rm cm}^{-1}$.

A single minimization process could lead to a local minimum; this risk was avoided by repeating the procedure several times with different initial geometries. In practice we started with a set of initial geometries obtained by generating points in a cube with a pseudo-random-number generator. We used the following constraint to eliminate very unlikely geometries: If a new generated point was near an already existing point or too far from all the previously generated points, it was discarded.

Within 10 to 15 relaxation steps the energy converges to within a few hundredths of an eV, the cluster symmetry,

if any, is clearly recognizable, but the internuclear distances are still 0.2 to 0.3 a.u. from convergence. After collecting the data from the relaxation of a dozen different initial geometries, we can clearly identify the equilibrium geometry of the cluster and the geometries of some local minima.

We then generate a second set of initial cluster geometries which include (i) the geometry with the symmetry of the absolute minimum and of some of the lowest local minima identified with the relaxation of the first set, (ii) the highly symmetric geometries of the cluster that cannot be ruled out by a Jahn-Teller analysis, (iii) other geometries and symmetries quoted in the literature. The geometrical parameters which are not determined by the symmetry constraints are again chosen at random, and a few different geometries are generated for each case. When these clusters are allowed to relax under the action of the Hellmann-Feynman forces, they automatically conserve their symmetry and, since there are just a few free parameters, an excellent convergence in energy and geometry is achieved within ~ 10 minimization steps. The results obtained with the first set have always been confirmed by the second set.

The probability of finding a local minimum formed by weakly interacting smaller units becomes significant for clusters with 7 and 8 atoms when the initial geometry is chosen at random; it becomes dominant for the 13-atom cluster. This limits the efficiency of our minimization method for the larger clusters. Therefore, in the case of Na_{13} and Na_{13}^+ we studied only some Jahn-Teller distortions of the highly symmetric icosahedral and cubooctahedral configurations.

III. RESULTS

As a test of the precision that can be expected from the pseudopotential local-spin-density method used in this calculation, we compare in Table II the well-known experimental spectroscopic constants of Na_2 and Na_2^+ with our theoretical results. As can be seen, the calculated equilibrium distances of Na_2 and Na_2^+ are 5% shorter than the measured values and the dissociation energies are 5 to 20% larger than the measured values. We thus expect, as a general rule, that the interatomic distances will be underestimated and that the binding energies will be overestimated throughout the calculations.

The deviation with respect to the experimental results is larger with the *ab initio* pseudopotential used in this work than with the empirical pseudopotential used in a previous work,[4] where a discussion of the accuracy of the LSD approximation and of the empirical pseudopotential can be found.

TABLE II. Experimental and calculated spectroscopic constants of the neutral and ionized sodium dimers. The equilibrium distance r_e is given in atomic units, the dissociation energy in eV, and the vibrational frequency ω_e in cm^{-1}.

		Experimental	Calculated
Na_2	r_e	5.818[a]	5.48
	D_e	0.747±0.001[a]	0.91
	ω_e	159.1[a]	173
Na_2^+	r_e	6.72[b]	6.42
	D_e	0.991±0.001[c]	1.05
	ω_e	119[b]	115

[a]Reference 56.
[b]Reference 50.
[c]Value obtained using the data of Refs. 49, 50, and 56.

A. Equilibrium geometries

The equilibrium geometries of neutral and ionized clusters having $n \leq 8$ and $n = 13$ atoms are given in Figs. 1, 2, 4, and 5. We have also added in Fig. 3 the geometries of the lowest-lying local minima of Na_6 and Na_6^+.

The equilibrium geometry of the Na_3 trimer (Fig. 1) is an isosceles triangle (C_{2v} symmetry) with an apex angle of 78°; it is a Jahn-Teller distortion of an equilateral triangle geometry. The equilibrium geometry of the Na_3^+ molecule (Fig. 2) is an equilateral triangle (D_{3h} symmetry). A calculation of the whole Born-Oppenheimer surface of Na_3 using the same method but an empirical pseudopotential, has been reported in a previous paper.[4] We discussed there the dynamical character of the Jahn-Teller effect and we compared the trimer results with the available experimental and theoretical results.

Both the Na_4 (Fig. 1) and the Na_4^+ (Fig. 2) clusters have a rhombic equilibrium geometry (D_{2h} symmetry). Similar equilibrium geometries have been previously obtained with the same pseudopotential local-spin-density

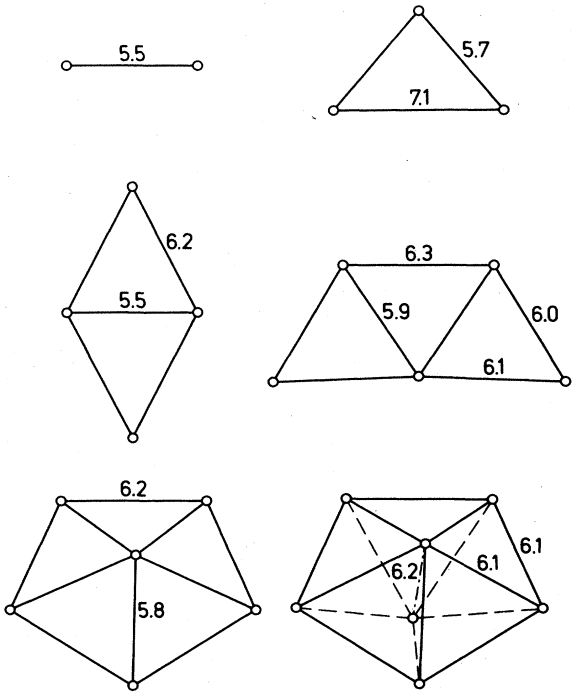

FIG. 1. Equilibrium geometries of Na_n clusters with $n \leq 7$. The internuclear distances are given in atomic units.

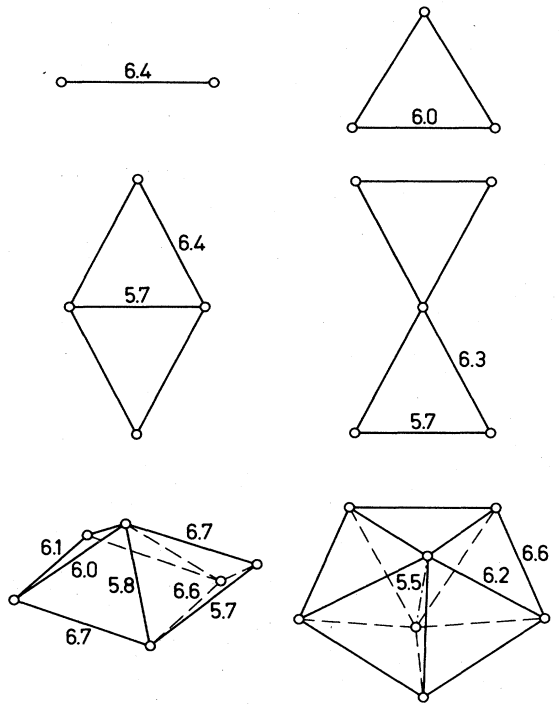

FIG. 2. Equilibrium geometries of Na_n^+ clusters with $n \leq 7$. The internuclear distances are given in atomic units.

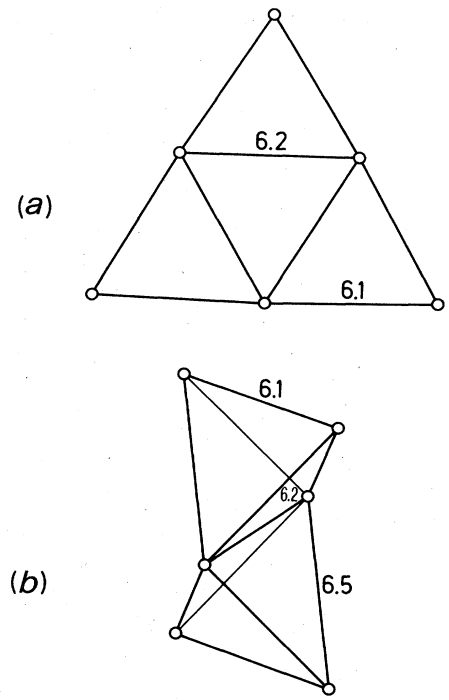

FIG. 3. Geometries of the isomers of the (a) Na_6 and (b) Na_6^+ clusters with lowest energy. The interatomic distances are given in atomic units.

method[43] and with other methods.[25,26] In this calculation we have identified several minima on the Born-Oppenheimer surface which are more than 0.15 eV higher in energy than the true minimum.

The Na_5 cluster has a planar equilibrium geometry (Fig. 1) with an almost trapezoidal shape (C_{2v} symmetry) formed of three slightly distorted equilateral triangles. All the other local minima, including the triangular bipyramid,[25] the "dagger" structure[25] and the quadrangular pyramid are, more than 0.15 eV higher in energy than the trapezoidal equilibriam geometry. The Na_5^+ equilibrium geometry is composed of two iscosceles triangles with a common apex (D_2 symmetry). They can rotate almost freely with respect to the axis joining the apex atom to the middle point of the bases of the triangles. The special case of a plane geometry (D_{2h} symmetry) is shown in Fig. 2; another particular geometry has the D_{2d} symmetry. When the free rotation is taken into account, we expect the effective geometry of this cluster to have a $D_{\infty h}$ symmetry. Furthermore, the bending modes of one triangle with respect to the other are very soft.

The equilibrium geometry of Na_6 (Fig. 1) is a pentagonal pyramid (C_{5v} symmetry) flattened with respect to the regular pyramid where all the edges are of the same length. The energy surface of Na_6 has a local minimum lying only 0.04 eV above that of the pentagonal pyramid. The geometry of this isomer is given in Fig. 3; it is a planar structure formed by a central equilateral triangle surrounded by three isosceles triangles (D_{3h} symmetry). Similar geometries were found to be the most stable in a configuration interaction study of Li_6 (Ref. 27) in which the interatomic distances were kept at the bulk value. The geometry of Na_6^+ (Fig. 2) has a very low symmetry (C_s) although it can be described as a distortion of a bcc-like structure. The Na_6^+ energy surface has a local minimum with D_{2h} symmetry (Fig. 3), which is also very close in energy (0.03 eV) to the absolute minimum.

Both the Na_7 (Fig. 1) and Na_7^+ (Fig. 2) clusters have a pentagonal bipyramidal structure (D_{5h} symmetry), but whereas Na_7 has an almost regular structure where all edges have approximately the same length, the structure of Na_7^+ is flattened with respect to a regular bipyramid.

The equilibrium geometries of Na_8 and Na_8^+ (Fig. 4) have rather compact structures with respectively, the D_{2d} and C_{2v} symmetries. The geometry of Na_8^+ is a slight distortion of a bcc-like structure and can be obtained from the Na_8 geometry through a relatively large distortion.

The equilibrium geometries of Na_{13} and Na_{13}^+ (Fig. 5) were obtained by studying a few symmetrical distortions of the cubo-octahedron and of the icosahedron, in contrast with the calculation of the equilibrium geometries of the other clusters, where no *a priori* geometry was assumed. We find, both for Na_{13} and Na_{13}^+, that the energy minima are slight distortions of the cubo-octahedron with D_{4h} symmetry. If we force the cluster symmetry using fractional occupation numbers we find that the cubo-octahedron is 0.2 eV more stable than the icosahedron. Recently a configuration interaction (CI) calculation for the Li_{13} cluster[29] suggested that its equilibrium geometry is an icosahedron with a sextuplet ground state whereas our distorted cubo-octahedron has a doublet ground state. The possible existence of alkali clusters with a high-spin

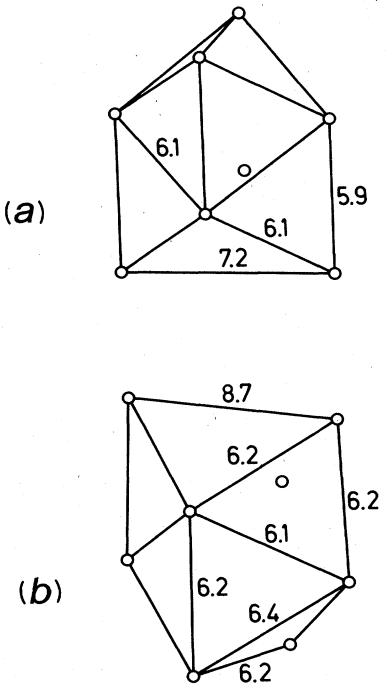

FIG. 4. Equilibrium geometries of (a) Na_8 and (b) Na_8^+ clusters. The interatomic distances are given in atomic units.

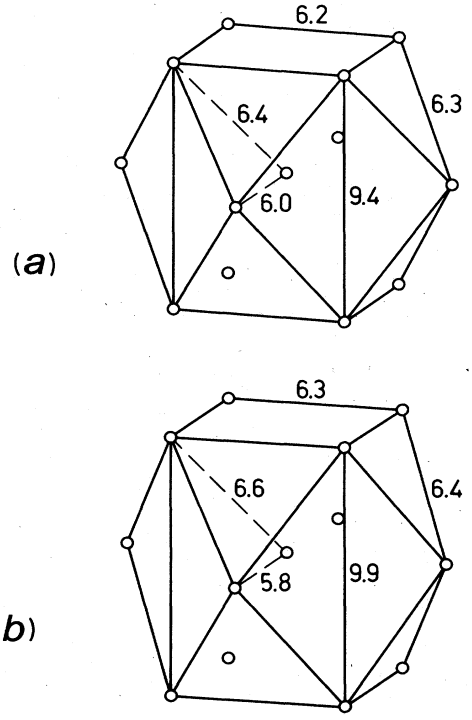

FIG. 5. Equilibrium geometries of (a) Na_{13} and (b) Na_{13}^+ clusters. The interatomic distances are given in atomic units.

ground state is worth considering since magnetic Stern-Gerlach experiments have been performed on these clusters.[44] The ground state of the highly symmetric icosahedral configuration is a sextuplet and is stable with respect to distortions, whereas there is always a distortion that lowers the energy of degenerate, lowest lying, doublet state. An equilibrium configuration with doublet ground state results when the lowering in energy obtained with a Jahn-Teller distortion is larger than the magnetic energy gained by having the five spins aligned in the sextuplet state.

The CI and the LSD methods differ essentially by their treatment of the exchange and correlation interactions. While the LSD scheme treats both in the *same* approximate way, the CI method treats the exchange essentially exactly but the description of the correlation interaction depends strongly on the completeness of the CI expansion. For large molecules, where size consistency effects are present, only a fraction of the correlation energy is usually recovered in the CI calculations. Since the correlation interaction reduces the preference of the exchange interaction for an high-spin ground state, CI calculations with an incomplete CI expansion can predict an high-spin ground state for a molecule with a low-spin ground state.

We give in Table III some results concerning the interatomic distances deduced from this calculation. The smallest interatomic distance $R_{\min}$ increases slowly towards the bulk value with growing cluster size, whereas no clear trend appears in the average value $\langle R \rangle$ of the nearest-neighbor distances. For large-size clusters the experimental results[1] suggest that the interatomic distances within a cluster decrease with respect to the infinite solid by an amount proportional to $n^{-1/3}$, where n is the number of atoms, in agreement with the prediction of a classical drop model[1,45] that explains the cluster contraction as a surface-tension effect. The size range we have studied, 2 to 13 atoms, is too small to allow an extrapolation of the asymptotic behavior.

The variance of the nearest-neighbor distances strongly decreases with increasing cluster size (Table III), already

TABLE III. Distances between nearest-neighbor atoms in the sodium clusters. $R_{\min}$, $\langle R \rangle$, and ΔR are, respectively, the smallest interatomic distance, the average value, and the variance of the nearest-neighbor distances. All values are given in atomic units, the experimental values are given in parentheses.

	$R_{\min}$	$\langle R \rangle$	ΔR
Na_2	5.5(5.8[a])	5.5	
Na_3	5.7	6.2	0.69
Na_4	5.5	6.0	0.32
Na_5	5.9	6.0	0.13
Na_6	5.8	6.0	0.20
Na_7	6.1	6.1	0.04
Na_8	5.9	6.0	0.05
Na_{13}	6.0	6.3	0.11
Na_∞ (bulk)	(6.9[b])		

[a]Reference 56.
[b]Reference 58, p. 31.

reflecting the onset of the regularity of the cluster structures in these very small aggregates. The larger variance for the Na_{13} clusters could be an indication that the cubo-octahedron is a local minimum and not the absolute minimum of the energy surface.

The equilibrium geometries we have obtained for clusters larger than four atoms are different from those found by Flad *et al.*,[25] who studied only some symmetrical cluster configurations. We have also checked that all our geometries have a lower energy than the structures found by Flad *et al.*

Our results can be summarized as follows: (i) Sodium clusters with five atoms or less have a planar structure built from distorted equilateral triangles, which is the typical pattern of close packing in two dimensions. (ii) The aggregates with six, seven, and eight atoms have three-dimensional structures (although those with six electrons or less are flattened with respect to an ideal geometry) and a regularity of the interatomic distances starts to appear. (iii) A slight distortion of the cubo-octahedron rather than an icosahedral structure appears to be a lower-energy configuration for both 13-atom clusters.

B. Ionization potentials

The appearance potential of Na_n clusters in a molecular beam have been measured by photoionization followed by mass spectroscopy.[14–16] In a clean experiment, where no fragmentation or multiphoton processes occur and where the distribution of the excited states is approximately Boltzmannian, the appearance potentials of the clusters are equal to the adiabatic ionization potentials.[14,46]

We show in Fig. 6 the calculated adiabatic ionization potentials of Na_n clusters and the experimental values of Herrmann *et al.*[14] and Peterson *et al.*[15] In this figure we have also drawn the results of a simple electrostatic model.[45,47,48] More accurate adiabatic ionization potentials have been obtained from the Rydberg spectra of Na,[49] Na_2,[50] and Na_3,[51] giving, respectively, the values 5.139, 4.895, and 3.92 eV. The agreement between the values of the two different experiments[14,15] is not very good for the Na_5, Na_6, and Na_8 clusters. Our calculated ionization potentials, and in particular their trend, are in better agreement with the results of Herrmann *et al.* Since our method is *ab initio,* parameter free, and describes correctly the ionization potentials for the smallest Na_n clusters, the better agreement with the results of Herrmann *et al.* could indicate that these are more accurate. When we compare the calculated vertical ionization potentials with the experimental appearance potentials we find poor agreement, confirming the interpretation of the appearance potentials as adiabatic ionization potentials.[14] Previous calculations of the ionization potentials of Na_n clusters have been reported by Flad *et al.*;[25] they have, however, calculated vertical ionization potentials of selected cluster structures, which we believe cannot be directly compared with the experimental appearance potentials.[52]

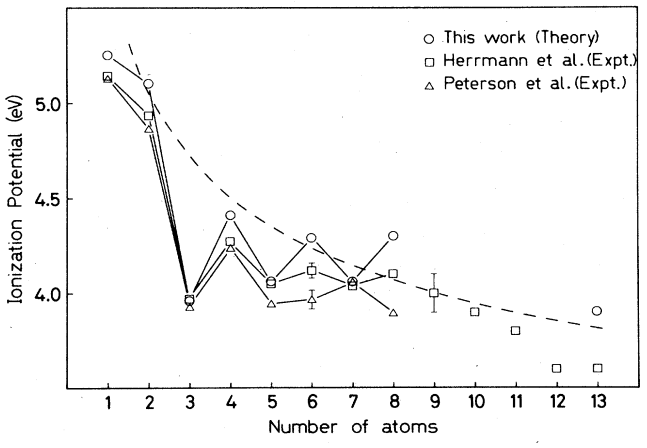

FIG. 6. Ionization potentials of Na_n clusters. The circles are the calculated adiabatic ionization potentials, the squares and the triangles are, respectively, the photoionization appearance potentials of Refs. 14 and 15. We have only shown the experimental error bars for the Na_6 and Na_9 cases. The broken line is the result of a simple electrostatic model.

C. Comparison with ESR experiments

The electron-spin-resonance (ESR) spectra of alkali clusters trapped in a frozen inert-gas matrix have been reported by Lindsay and co-workers.[20,21,53,54] They have observed spectral features which they assign to atoms, trimers, and septamers, the spectra of pentamers have, however, not been identified. Clusters with an even number of atoms have a singlet ground state and therefore cannot be observed in ESR experiments.

Interpretation of the hyperfine structure of the ESR spectra gives the electronic spin density at the nuclear sites, which is often expressed as a fraction of the atomic value and denoted the isotropic spin population. At low temperatures the ESR spectra attributed to Na_3 have large and equal spin densities at two nuclear sites and a smaller spin density with opposite sign at a third nucleus. At temperatures higher than 20 K, an ESR signal where all three atoms have the same spin density appears.[54] Our calculated charge and spin density for the equilibrium geometry of Na_3 (Fig. 7) are consistent with the low-temperature spectra; the high-temperature spectra have been previously explained by the pseudorotation of the Na_3 molecule.[4,54] The ESR signal attributed to the Na_7 molecule has large and equal spin densities at two atoms and a smaller spin density at five other equivalent atoms.[21,55] These results are consistent with a pentagonal bipyramidal equilibrium geometry for Na_7,[21] and the calculated charge and spin densities given in Fig. 8 are in agreement with the experimental result. We thus compare in Table IV the measured isotropic spin populations and the calculated "pseudo" isotropic spin populations for Na_3 and Na_7. We also report in Table IV the pseudo isotropic spin populations, computed from the charge and spin density of the trapezoidal Na_5 cluster (Fig. 9). The agreement between theory and experiment is excellent for Na_3 and Na_7; the calculated values for Na_5 can help to identify the ESR spectrum of Na_5 which is yet unknown.

In our calculation we compute pseudo spin densities rather than real spin densities at the nuclear sites. This

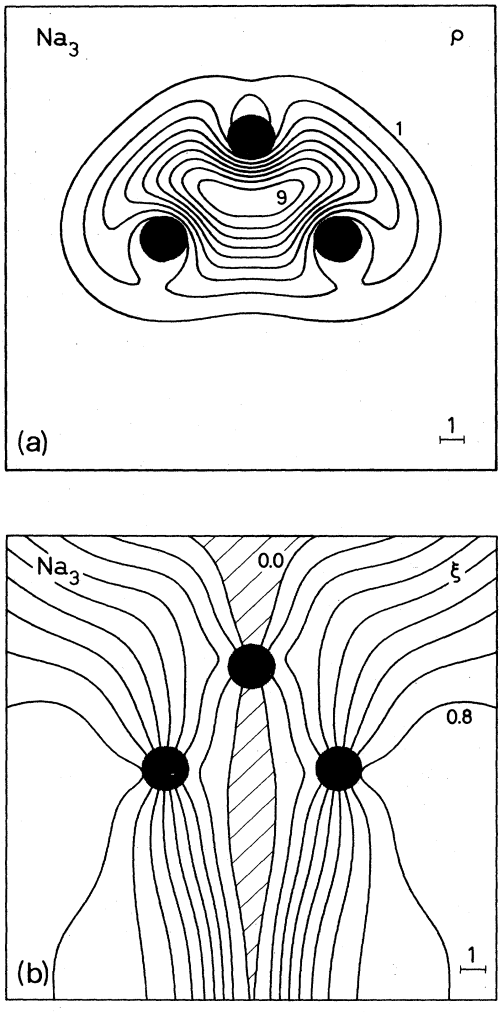

FIG. 7. Contour plots of the (a) electronic charge density and (b) spin density parameter of Na_3 on the plane of the three atoms. The length scale is given in atomic units at the lower right corner of the figure in a.u. (Bohr), the charge density is given in units of 10^{-3} electron per cubic atomic unit. The shaded areas show the extension of the atomic cores.

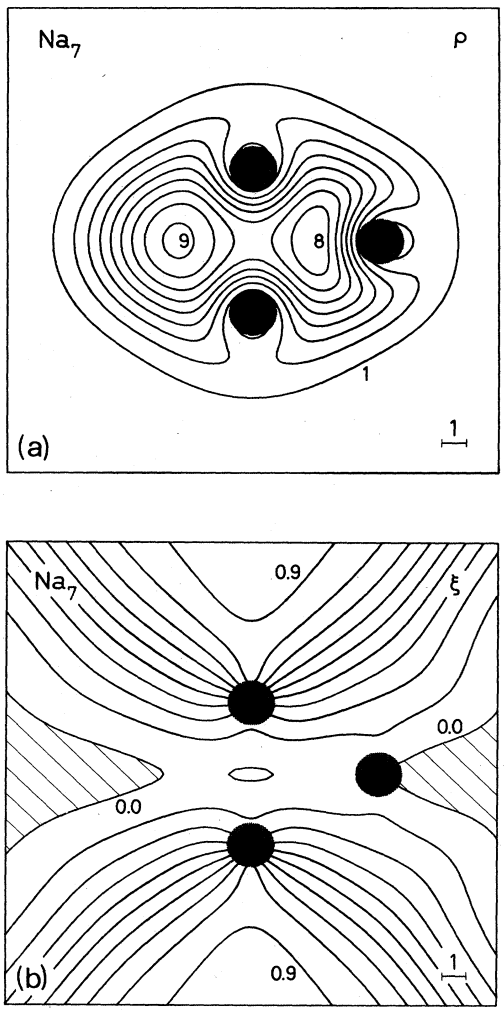

FIG. 8. Contour plots of the (a) electronic charge density and (b) spin density parameter of the Na_7 cluster in one of the five vertical symmetry planes of the D_{5h} symmetrical point group. The units are the same as in Fig. 7.

should affect only minimally the calculated isotropic spin populations, since both the real and the pseudo isotropic spin populations are normalized to their corresponding atomic values, and both are a measure of the strength of the *s* part of the unpaired electron wave function at each nucleus.

The matrix results should be extrapolated with care to the intrinsic properties of the isolated clusters. For example, the *g* shift depends on the matrix site, however the spin populations are relatively unaffected by matrix-site effects or even by the matrix material itself.[21]

D. Dissociation and atomization energies

The calculated atomization energies per atom of the sodium clusters (Table V) converge smoothly to their bulk value, i.e., the binding energy per atom of the solid,

TABLE IV. Experimental isotropic spin populations and calculated "pseudo" isotropic spin populations. The multiplicity of each value is indicated in parentheses.

	Experimental	Calculated
Na	1.0	1.0
Na_3	0.47[a](2×)	0.48(2×)
	−0.07	−0.04
Na_5	b	0.19(2×)
		0.17(2×)
		0.06
Na_7	0.37(2×)[c]	0.32(2×)
	±0.02(5×)	−0.02(5×)

[a]Reference 20.
[b]The ESR spectra of Na_5 has not been observed.
[c]Reference 21.

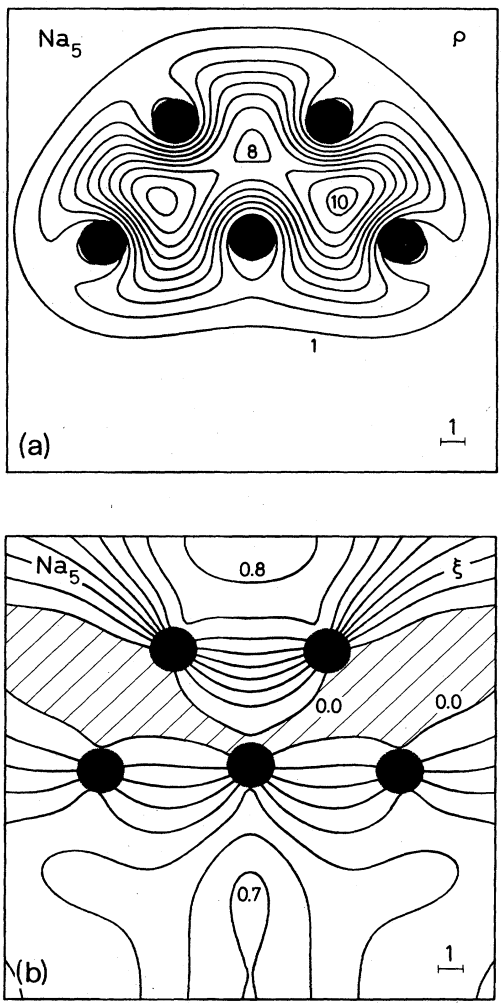

FIG. 9. Contour plots of the (a) electronic charge density and (b) spin density parameter of the Na_5 cluster on the plane containing the five atoms. The units are the same as in Fig. 7.

whereas the dissociation energies (Table VI) show a more irregular convergence which reflects their stronger dependence on the structure of the clusters. In order to obtain the dissociation energies, we analyzed all the possible dissociation channels of the clusters. For both the neutral and the ionized clusters the first dissociation channel is given by

$$Na_n^{(+)} \rightarrow Na + Na_{n-1}^{(+)} ,$$

with the exception of Na_4 and Na_6 which dissociate into a neutral dimer and a $n-2$ atom cluster.

The experimental values of the dissociation energies of Na_2 have been obtained by fluorescence spectroscopy[56] and from the thermochemical data of sodium vapor in a Knudsen cell,[57] for Na_3 only the less precise Knudsen-cell result is known.[57] From these values and the experimental ionization potentials we have derived the experimental dissociation energies for Na_2^+ and Na_3^+ given in Table VI. As we already observed in the dimer case, our pseudopotential local-spin-density approach gives larger binding energies for the neutral and ionized trimers than the experimental values (Tables V and VI). We also notice that the calculated dissociation energies for the ionized clusters (Table VI) are of the order of 1 eV, therefore the excess energy needed to break a cluster by photoionization[17] is fairly high.

TABLE V. Atomization energies per atom of the sodium clusters. The values in parentheses are the experimental values. All energies are given in eV.

Na_2	0.45(0.37[a])	Na_2^+	0.52(0.45[b])
Na_3	0.43(0.36[c])	Na_3^+	0.86(0.76[b])
Na_4	0.61	Na_4^+	0.82
Na_5	0.64	Na_5^+	0.88
Na_6	0.73	Na_6^+	0.89
Na_7	0.82	Na_7^+	0.99
Na_8	0.86	Na_8^+	0.97
Na_{13}	0.86	Na_{13}^+	0.96
Na_∞ (bulk)	(1.11[d])		(1.11[d])

[a]Reference 56.
[b]Values obtained using the data of Refs. 49, 50, 51, 56, and 57.
[c]Reference 57.
[d]Reference 58, p. 74.

IV. DISCUSSION

The distinction between metallic and covalent bonding is less marked in molecules or very small aggregates than in macroscopic condensed matter since the concept of a band gap cannot be precisely defined in a molecule or small cluster. If we accept the distinction that metallic bonding is weak, nonlocalized, and nondirectional whereas covalent bonding is strong, localized in the bond region, and directional,[58] this study shows that the sodium clusters are typical cases of metallic bonding. Such metallic bonding in a sodium cluster is to be expected since it is known that the ions act as weak scatterers in the bulk

TABLE VI. Dissociation energies in eV of the sodium clusters. The values in parentheses are the experimental values.

Na_2	0.91(0.747±0.001[a])	Na_2^+	1.05(0.991±0.001[b])
Na_3	0.40(0.33[c])	Na_3^+	1.55(1.30[b])
Na_4	0.63	Na_4^+	0.68
Na_5	0.76	Na_5^+	0.88
Na_6	1.03	Na_6^+	0.95
Na_7	1.35	Na_7^+	1.63
Na_8	1.14	Na_8^+	0.88
Na_∞ (bulk)	(1.11[d])		(1.11[d])

[a]Reference 56.
[b]Values obtained using the data of Refs. 49, 50, 51, 56, and 57.
[c]Reference 57.
[d]Reference 58, p. 74.

metal; this is confirmed by the delocalized character of the bonding charge (Fig. 10). In their work, however, Flad *et al.*[25] reached the conclusion that the structures with Na_2 units are a characteristic feature of small sodium clusters. This dimerization would mean that weakly localized and directional bonds are formed between pairs of atoms, a situation that can be described as a covalent contribution to the bonding. Qualitative theoretical arguments[59] also indicate a possible dimerization if the mean coordination number is smaller than 4. In our work we find no sign of dimerization.

In the tight-binding picture of metallic bonding, structures with a large number of nearest neighbors are favored since their bandwidths are larger.[59] Our calculated equilibrium geometries of Na aggregates do not, however, always maximize the number of nearest neighbors. For example, the clusters with five atoms or less have a plane geometry made from distorted equilateral triangles. The equilateral triangle is indeed the building block of close packing in two dimensions, but the number of nearest neighbors would be increased if the four- and five-atom clusters had the shape of the tetrahedron and a triangular bipyramid, respectively. Another example is given by the Na_6 cluster, whose pentagonal pyramid geometry has fewer nearest neighbors than the more compact octahedral geometry.

The fundamental reason why the most symmetrical structures are not favored by small sodium clusters is their instability with respect to a Jahn-Teller distortion. The Jahn-Teller theorem asserts that a nonlinear molecule cannot have a degenerate ground state (except for simple Kramers degeneracy) since there is always a symmetry-breaking distortion which lowers the energy.[60] The highly symmetric geometries possess a high probability of having a degenerate ground state and therefore are discriminated against the Jahn-Teller effect in favor of geometries with lower symmetry.

In order to understand the geometrical structure of small clusters, we have thus to take a closer look at their electronic structure and study how it changes with increasing number of electrons, taking into account the delocalized character of the valence electrons. The main point for sodium clusters is to realize that the molecular orbitals, which are essentially linear combinations of the $3s$ atomic orbitals, can be classified as "s like", "p like", "d like", etc., according to their global shape (Fig. 11). They are filled in a well-defined order as the number of electrons in the cluster increases. This classification can be justified in a more formal way since these molecular orbitals generate the same representation of the symmetries of the molecule as a set of functions with well-defined angular momentum.

For the clusters with one and two valence electrons, a single nodeless s-like orbital[61] is occupied. This orbital has a tendency to be spherical in order to lower its kinetic energy; the ions will thus try to adjust to this spherical shape and tend to form a compact structure. Na_2 and Na_2^+ can only be linear, but Na_3^+ is an equilateral triangle, the most compact geometry for a trimer.

As we add the third and the fourth electrons, the next occupied orbital must be orthogonal to the first. It has a nodal surface separating two semi-infinite half-spaces, in which the orbital has different signs; it is an example of a p-like orbital. There are, however, three p-like orbitals

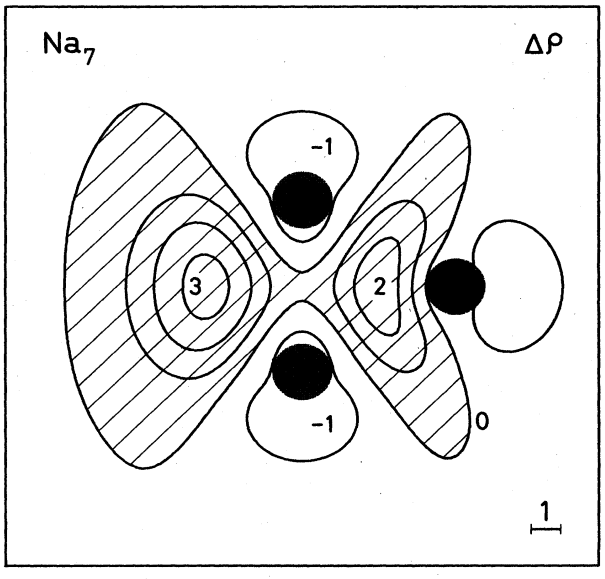

FIG. 10. Contour plots of the bonding charge (molecular charge density minus the sum of atomic charge densities) in the Na_7 cluster, showing the delocalized character of the metallic bond. The units are the same as in Fig. 7, the represented plane is the same as in Fig. 8, and the lightly shaded areas show the regions of charge accumulation.

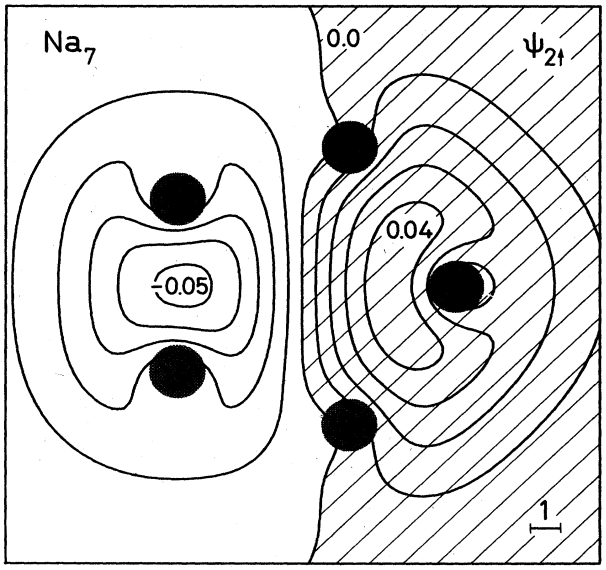

FIG. 11. Example of a p-like molecular orbital in the Na_7 cluster, represented in the plane containing five atoms.

and degeneracies can occur in a high-symmetry cluster, which could thus be subject to a Jahn-Teller distortion. If, to give a specific example, we want to study the stability with respect to Jahn-Teller distortions of the Na_4 cluster with a tetrahedral shape (T_d symmetry), we need only know that $\{x,y,z\}$ form the T_2 irreducible representation of the cubic group T_d, which implies that the three p-like orbitals are degenerate. The Na_4 molecule with two electrons in the s-like, fully symmetrical (A_1 irreducible representation) molecular orbital, and two electrons in the three degenerate p-like orbitals (T_2 irreducible representation) has a degenerate electronic ground state and is therefore unstable with respect to Jahn-Teller distortions. The stable molecules have one s-like and one p-like orbital occupied, so the electronic charge density tends to have the shape of a prolate ellipsoid of revolution. The ions will move to stabilize this shape, which leads to an elongated structure. This is the case for Na_3, Na_4, Na_4^+, and Na_5^+.

A fifth electron will occupy a second p-like orbital giving a situation in which the first p-like orbital is doubly occupied, the second is singly occupied and the third is empty. Since in this case there can be no degeneracies, the only allowed symmetries are the D_{2h} group and its subgroups. The Na_5 and Na_6^+ clusters have, indeed, a very low symmetry.

The clusters with six electrons have one s-like and two p-like orbitals fully occupied. In this case the two occupied p-like orbitals can be degenerate and the charge density tends to take the shape of an oblate ellipsoid of revolution. The molecule can thus have a high-order symmetry axis perpendicular to the plane of the two occupied p-like orbitals; this is the case for Na_6 and Na_7^+, which have a fivefold symmetry axis. The geometries of these clusters are flattened compared to the regular pyramid and bipyramid, in which all edges would be equal. This is the result of a compromise between the four electrons in the p-like orbitals, which prefer a planar geometry, and the two electrons in the s-like orbitals, which favor a compact geometry. The isomer of Na_6 with plane geometry reflects the same tendency.

The Na_7, Na_8, and Na_8^+ clusters, whose p-like orbitals are all occupied, have very regular three-dimensional configurations with their nearest-neighbor distances almost identical. In the 13-atom clusters the next available energy levels are d-like orbitals which are occupied by four or five electrons. These orbitals are fivefold degenerate in the icosahedron and are split into a threefold and twofold degeneracy in the cubo-octahedron. In the cubo-octahedron the three degenerate orbitals ("d_{xy}," "d_{xz}," and "d_{yz}") are directed toward the surface atoms and have a lower energy than the doubly-degenerate orbitals ("$d_{2z^2-x^2-y^2}$" and "$d_{x^2-y^2}$"), which are directed toward the square faces. Thus both the icosahedral and the cubo-octahedral geometries of Na_{13} and Na_{13}^+ are unstable if they have a low-spin configuration. The calculated equilibrium geometries of these clusters are Jahn-Teller distortions of the cubo-octahedron with the D_{4h} symmetry.

These results are interesting since molecular-dynamics calculations using additive two-body potentials always favor the most compact structures, i.e., icosahedral structures, for small clusters.[59] Experiments have also shown the presence of fivefold symmetry axes in clusters of rare gases and of noble metals[1,59] having fewer than 1000 atoms. Our results are not an indication that bulk like (fcc) structures are already attained with 13 atoms for alkali metal clusters, but rather suggest a manifestation of the Jahn-Teller effect. The importance of the incompletely filled molecular shells will decrease as a function of the cluster size, and we cannot exclude the dominance of icosahedral structures for larger clusters.

This analysis shows that the electronic structure is the principal factor which governs the equilibrium geometry of the clusters and that the main features of the electronic structure are fairly insensitive to the actual geometrical structure. In fact the s-like, p-like, and d-like ordering of the energy levels has been previously found in a spherical jellium model of Na clusters in which the ions were replaced by a spherical background of charge.[45] In that model the ordering of the energy levels was $s,p,d,s,f,p,g,d,h,s,f,\ldots$. Recently a similar shell structure was used to explain a mass spectrum of sodium clusters produced in a molecular beam, where each significative drop in the ion signal occurred just after a shell was completed.[62]

A complete study of the equilibrium geometry of the clusters should take into account dynamical Jahn-Teller effects. Generally speaking, we cay say that if the distortions are smaller than the typical zero-point vibration amplitudes of sodium molecules (~ 0.2 a.u.) as in, for instance, the case of Na_{13}, then the molecular vibrational wave function is not localized within each of the equivalent potential minima of the energy surface, and the effective cluster geometry has the same symmetry as the undistorted cluster. We expect this to be the case for the larger clusters, where the importance of the incompletely filled molecular shells will decrease, and therefore result in smaller Jahn-Teller distortions. If the distortions are large, as in the case of Na_4, viewed as a Jahn-Teller distortion of a square, then the equivalent minima on the Born-Oppenheimer are well separated in space, with large potential barriers between them. In this case the interaction between the equivalent minima can be neglected and the effective geometry is the distorted geometry. The Na_3 molecule is a special case where the Jahn-Teller distortion is comparable to the zero-point vibrational amplitude. The barrier between the equivalent minima is of the order of 0.03 eV (Ref. 4) and, depending on the cluster temperature and on the time scale of the measured property, an isosceles or an equilateral triangle geometry should be observed.[4,54]

V. CONCLUSION

Realistic calculations of the electronic and structural properties of Na_n clusters with n as large as 13 have been performed in the framework of the pseudopotential and local-spin-density approximations. The equilibrium geometries of the clusters have been obtained by allowing randomly generated clusters to relax under the action of the Hellmann-Feynman forces.

We find the bondings to be weak, delocalized, and non-

directional, which is a characteristic of a metallic bonding. The structures are closely packed, either in two dimensions for clusters with five atoms or less, or in three dimensions for the larger clusters, but do not always maximize the number of nearest neighbors. The tendancy toward dimerization reported in a previous study was not observed. A model has been given to explain the equilibrium shape of the very small clusters of simple metals. It takes into account the *s*-, *p*-, and *d*-like global shape of the molecular orbitals of the clusters.

The atomization energy per atom increases smoothly toward the bulk value with increasing particle size whereas the dissociation energy shows a more irregular convergence. The smallest internuclear distance also increases with increasing particle size, but the variance of the internuclear distances decreases dramatically. This shows that the onset of regularity already appears for very small clusters.

These theoretical results have been compared with the available experimental data. In particular, the calculated adiabatic ionization potentials are in good agreement with the measured appearance potentials of Herrmann *et al.*,[14] and the calculated equilibrium geometries and wave functions of Na_3 and Na_7 are in excellent agreement with the spin densities deduced by ESR on Na_3 and Na_7 clusters trapped in an inert-gas matrix. We present also a prediction for the isotropic spin densities relevant to the ESR spectra of Na_5, which has not yet been observed.

*Present address: Solar Energy Research Institute, Golden, Colorado 80401.

[1]S. Ino, J. Phys. Soc. Jpn. **21**, 346 (1966); C. Solliard, Ph.D. thesis, Ecole Polytechnique Fédérale de Lausanne (EPFL), 1983.

[2]J. H. Sinfelt, Rev. Mod. Phys. **51**, 569 (1979).

[3]*The Theory of the Photographic Process,* edited by T. H. James (MacMillan, New York, 1977); J. F. Hamilton, in *Growth and Properties of Metal Clusters, Application to Catalysis and the Photographic Process,* edited by J. Bourdon (Elsevier, New York, 1980).

[4]J. L. Martins, R. Car, and J. Buttet, J. Chem. Phys. **78**, 5646 (1983).

[5]W. H. Gerber and E. Schumacher, J. Chem. Phys. **69**, 1692 (1978).

[6]O. Gunnarsson and B. I. Lundqvist, Phys. Rev. B **13**, 4274 (1976).

[7]P. Hohenberg and W. Kohn, Phys. Rev. B **136**, 864 (1964); W. Kohn and L. J. Sham, Phys. Rev. A **140**, 1133 (1965).

[8]D. R. Hamann, M. Schlüter, and C. Chiang, Phys. Rev. Lett. **43**, 1494 (1979).

[9]G. B. Bachelet, D. R. Hamann, and M. Schlüter, Phys. Rev. B **26**, 4199 (1982).

[10]H. Hellmann, *Einführung in die Quantenchemie* (Deuticke, Leipzig, 1937); R. P. Feynman, Phys. Rev. **56**, 340 (1939).

[11]J. C. Slater, J. Chem. Phys. **57**, 2389 (1972).

[12]J. Ihm, A. Zunger, and M. L. Cohen, J. Phys. C **12**, 4409 (1979).

[13]J. L. Martins, J. Buttet, and R. Car, Phys. Rev. Lett. **53**, 655 (1984).

[14]A. Herrmann, E. Schumacher, and L. Wöste, J. Chem. Phys. **68**, 2327 (1978).

[15]K. I. Peterson, P. D. Dao, R. W. Farley, and A. W. Castleman, Jr., J. Chem. Phys. **80**, 1780 (1984).

[16]P. J. Foster, R. E. Leckenby, and E. J. Robbins, J. Phys. B **2**, 478 (1969).

[17]G. Delacrétaz, J. D. Ganière, R. Monot, and L. Wöste, J. Appl. Phys. B **29**, 55 (1982).

[18]G. Delacrétaz, P. Fayet and L. Wöste, Ber. Bunsenges. Phys. Chem., **88**, 284 (1984).

[19]J. L. Gole, G. J. Green, S. A. Pace, and D. R. Preuss, J. Chem. Phys. **76**, 2247 (1982).

[20]D. M. Lindsay, D. R. Herschbach, and A. L. Kwiram, Mol. Phys. **32**, 1199 (1976).

[21]G. A. Thompson, F. Tischler, and D. M. Lindsay, J. Chem. Phys. **78**, 5946 (1983).

[22]M. Hoffmann, S. Leutwyler, and W. Schulze, Chem. Phys. **40**, 145 (1975); T. Welker and T. P. Martin, J. Chem. Phys. **70**, 5683 (1979).

[23]F. W. Froben and W. Schulze, Ber. Bunsenges Phys. Chem. **88**, 312 (1984).

[24]R. L. Martin and E. R. Davidson, Mol. Phys. **35**, 1713 (1978).

[25]J. Flad, H. Stoll, and H. Preuss, J. Chem. Phys. **71**, 3042 (1979).

[26]H.-O. Beckmann, J. Koutecký and V. Bonacić-Koutecký, J. Chem. Phys. **73**, 5182 (1980); G. Pacchioni, H.-O. Beckman and J. Koutecký, Chem. Phys. Lett. **87**, 161 (1982).

[27]D. Plavšlć, J. Koutecký, and V. Bonacić-Koutecký, J. Chem. Phys. **87**, 1096 (1983).

[28]P. Fantucci, J. Koutecký, and G. Pacchioni, J. Chem. Phys. **80**, 325 (1984).

[29]G. Pacchioni and J. Koutecký, J. Chem. Phys. **81**, 3588 (1984).

[30]R. Car, R.-A. Meuli, and J. Buttet, J. Chem. Phys. **73**, 4511 (1980).

[31]J. L. Martins and W. Andreoni, Phys. Rev. A **28**, 3637 (1983); J. Harris and R. O. Jones, J. Chem. Phys. **68**, 1190 (1978); J. Bernholc and N. A. W. Holzwarth, Phys. Rev. Lett. **50**, 1451 (1983); B. Delley, A. J. Freeman, and D. E. Ellis, *ibid.* **50**, 488 (1983).

[32]B. Delley, D. E. Ellis, A. J. Freeman, E. J. Baerends, and D. Post, Phys. Rev. B **27**, 2132 (1983).

[33]J. P. Perdew and A. Zunger, Phys. Rev. B **23**, 5048 (1981).

[34]D. M. Ceperley and B. J. Alder, Phys. Rev. Lett. **45**, 566 (1980).

[35]J. L. Martins and R. Car, J. Chem. Phys. **80**, 1525 (1984).

[36]P. Pulay, in *Applications of Electronic Structure Theory, Modern Theoretical Chemistry,* edited by H. F. Shaeffer III (Plenum, New York, 1977), Vol. 4, p. 153.

[37]H. Nakatsuji, K. Kanda, and T. Yonezawa, J. Chem. Phys. **77**, 3109 (1982).

[38]P. Bendt and A. Zunger, Phys. Rev. Lett. **50**, 1684 (1983).

[39]H. B. Schlegel, in *Computational Theoretical Organic Chemistry,* edited by I. G. Csizmadia and R. Daudel (Reidel, Boston, 1981), p. 129.

[40]J. Ihm, M. T. Yin, and M. L. Cohen, Solid State Commun. **37**, 491 (1981); K. Kunc and R. M. Martin, Phys. Rev. Lett. **48**, 406 (1982); J. E. Northrup and M. L. Cohen, *ibid.* **49**, 1349 (1982).

[41]H. Sambe and R. F. Felton, J. Chem. Phys. **62**, 1122 (1975).

[42]J. L. Martins, Ph.D. thesis, Ecole Polytechnique Fédérale de

Lausanne, 1984.
[43]R. Car and J. L. Martins, Surf. Sci. **106**, 280 (1981).
[44]W. D. Knight, Helv. Phys. Acta **56**, 521 (1983).
[45]J. L. Martins, R. Car, and J. Buttet, Surf. Sci. **106**, 265 (1981).
[46]The appearance potential is the threshold of the energy of the ionizing particle (e.g., electron or photon) that produces a measurable ion signal. It can thus be sensitive to the experimental conditions. The true threshold for the ionization of a molecule in its ground state is the adiabatic ionization potential, which can be measured, for instance, from the study of the molecular Rydberg states. In a direct photoionization process, the Franck-Condon factor strongly favors vertical transitions corresponding to the vertical ionization potential, making difficult the measurement of the true ionization threshold. In the case of the alkali clusters, indirect transitions via the auto-ionizing Rydberg states contribute sufficiently to the total ion signal and the measured appearance potentials have been identified with the adiabatic ionization potentials. The experimental errors associated with the cluster temperature and the effect of the static electric fields are expected to be small (<0.01 eV). From a computational point of view the adiabatic ionization potential is the energy difference between the ground states of the neutral and the ionized clusters, whereas the vertical ionization potential is the energy difference between the ground state of the neutral cluster and the unrelaxed ionized cluster.
[47]D. M. Wood, Phys. Rev. Lett. **46**, 749 (1981).
[48]In the electrostatic model, to obtain the ionization potential of a spherical cluster of radius R we must add to the work function of the bulk metal the classical electrostatic energy of a charged metallic sphere, i.e., $1/2R$. A diverging expression is obtained if the energy is computed from the integration of the image force. This divergence can be removed by subtracting out the result for the flat surface, giving the value of $3/8R$. The image-force result seems to be in better agreement with the experimental results for sodium [E. Schumacher, M. Kappes, K. Marti, P. Radi, M. Schar, and B. Schmidhalter, Ber. Bunsenges. Phys. Chem. **88**, 220 (1984)].
[49]C. E. Moore, *Atomic Energy Levels*, Natl. Bur. Stand. (U. S.) Circular No. 467 (U. S. GPO, Washington, D. C., 1971).
[50]S. Leutwyler, T. Heinis, M. Jungen, H.-P. Härri, and E. Schumacher, J. Chem. Phys. **76**, 4290 (1982); S. Martin, J. Chevaleyre, S. Valignat, J. P. Perrot, M. Broyer, B. Cabaud, and A. Hoareau, Chem. Phys. Lett. **87**, 235 (1982).
[51]L. Wöste (private communication).
[52]Flad *et al.* have found reasonable agreement between their calculated vertical ionization potentials for selected geometries and the experimental appearance potentials. The agreement disappears when they compare the vertical ionization potentials of their equilibrium geometries.
[53]G. A. Thompson and D. M. Lindsay, J. Chem. Phys. **74**, 959 (1981); D. A. Garland and D. M. Lindsay, *ibid.* **78**, 2813 (1983).
[54]D. M. Lindsay and G. A. Thompson, J. Chem. Phys. **77**, 1114 (1982).
[55]The experimental evidence cannot rule out the possibility of having more than five atoms with a small spin density as is discussed in Ref. 21.
[56]K. K. Verma, J. T. Bahns, A. R. Rejei-Rizi, W. C. Stwalley, and W. T. Zemke, J. Chem. Phys. **78**, 3599 (1983).
[57]K. Hilpert, Ber. Bunsenges, Phys. Chem. **88**, 260 (1984).
[58]C. Kittel, *Introduction to Solid State Physics* (Wiley, New York, 1976).
[59]J. Friedel, Helv. Phys. Acta **56**, 507 (1983).
[60]M. Lax, *Symmetry Principles in Solid State and Molecular Physics* (Wiley, New York, 1974).
[61]We will consider only the nodes of the pseudo wave functions, i.e., we do not take into account the nodes imposed by the core orthogonality constraints. The number of nodes in the core region is not very important when discussing valence properties.
[62]W. D. Knight, K. Clemenger, W. A. de Heer, W. A. Saunders, M. Y. Chou, and M. L. Cohen, Phys. Rev. Lett. **52**, 2141 (1984).